

STUDY OF AN INCLINED INTERFACE OF CONTACT USING LATTICE BOLTZMANN METHOD

Oussama EL MHAMDI^{1*}, *Elalami SEMMA*¹

¹ Laboratory of engineering industrial management and innovation, University Hassan 1st, FST Settat, Morocco

*Corresponding author; oussama.elmhamdi@gmail.com

The lattice Boltzmann method and the particle image model are adopted to study a heat transfer problem with thermal contact resistance. In this paper, a new study involving an inclined interface of contact between two media is introduced in order to evaluate a two-dimensional heat transfer in the steady regime. A case of study and numerical results are provided to support this configuration. The obtained results show the effect of the thermal contact resistance on the heat transfer, as well as the temperature distribution on the two contacting media.

Key words: lattice Boltzmann method, thermal contact resistance, particle image model, inclined interface of contact

1. Introduction

The Lattice Boltzmann Method is a successful numerical modeling method based on the simulation of collision and streaming processes across a limited number of particles, which has an excellent stability and an important role in simulations of micro and macro fluid flows. Compared to the traditional CFD methods, LBM has many advantages especially in applications involving complex geometries and porous media. This method has proved its effectiveness in the field of conventional fluid flow and it has been used in many applications in simulating isothermal flows in the last years [1-3]. In addition, there have been studies aiming to construct a stable Thermal Lattice Boltzmann Method (TLBM) to solve heat transfer problems. He et al introduced a model based on a double population approach and which has a good numerical stability [4]. This model has been used by researchers to solve different thermo-hydrodynamic problems[5-7].

In heat transfer problems and more precisely, in modeling Thermal Contact Resistance (TCR), on the one hand, K. Han et al. introduced a novel numerical approach, the partial bounce back scheme (PBB), to account for thermal contact resistance between contacting surfaces within the framework of the thermal lattice Boltzmann method [8], and Chiyu Xie et al studied thermal conduction in composites with TCR [9]. On the other hand, M. El Ganaoui et al. introduced the Particle Image model (PI) which is a numerical approach for the thermal lattice Boltzmann method to solve problems with contact resistance between surfaces [10] and O. El Mhamdi and E.Semma established an overall comparison between these two models in order to determine the most accurate one [11].

The thermal contact resistance exists due to many reasons such as surface irregularities and impurities which represent a barrier to the normal circulation of heat flux. This phenomenon causes an interfacial gap between two contacting surfaces and has important impact in many applications like electronic packaging and composite materials design and manufacture. This practical applications explains the interest of these studies.

In this paper, we first show a presentation of the thermal lattice Boltzmann method, then we describe the main methodology of the Partial Bounce Back and Particle Image model. After that, we show the overall comparison between the two models, and finally we introduce our new study supported by a case of study and numerical results.

2. Thermal lattice Boltzmann method for two dimensional model

As said above, the Lattice Boltzmann Method consists on two steps, collision and streaming. These two steps are described by the following equations:

Collision:

$$f_i(x, y, t + \Delta t) = f_i(x, y, t) - (f_i(x, y, t) - f_i^{eq}(x, y, t)) \text{ for } 0 \leq i \leq n \quad (1)$$

Streaming:

$$f_i(x + \Delta x, y + \Delta y, t + \Delta t) = f_i(x, y, t + \Delta t) \text{ for } 0 \leq i \leq n \quad (2)$$

When n is the number of neighboring nodes

In the most used D2Q9 model, the particles at each node can remain at their positions or move their eight adjacent nodes as shown in Fig. 1. The nine discrete velocities of these movements e_i are given in eq.(3). And to each one corresponds a weighting coefficient w_i as given in eq. (4).

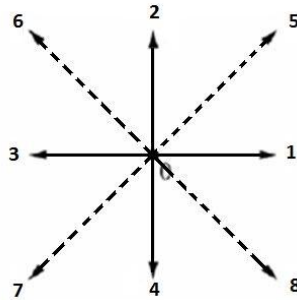


Figure 1. The nine possible vectors of movement for D2Q9 model

$$e_i = \begin{cases} 0 & \text{for } i = 0 \\ c(\pm 1, 0) \text{ and } c(0, \pm 1) & \text{for } 1 \leq i \leq 4 \\ c(\pm 1, \pm 1) & \text{for } 5 \leq i \leq 8 \end{cases} \quad (3)$$

Where c is the lattice speed, which is given by $c = \Delta x / \Delta t$ with Δx being the lattice spacing and Δt the time step.

$$w_i = \begin{cases} \frac{4}{9} & \text{for } i = 0 \\ \frac{1}{9} & \text{for } 1 \leq i \leq 4 \\ \frac{1}{36} & \text{for } 5 \leq i \leq 8 \end{cases} \quad (4)$$

The D2Q9 model allows to write:

Temperature

$$T(x, y, t) = \sum f_i(x, y, t) \quad \text{for } 0 \leq i \leq 8 \quad (5)$$

Flux

$$q = \sum e_i f_i(x, y, t) \quad \text{for } 0 \leq i \leq 8 \quad (6)$$

Where T and q are respectively the temperature and the heat flux at each node.

More precisely, in modeling Thermal Contact Resistance, two models have been introduced: the Partial Bounce Back model and the Particle Image model. In the following chapter, an overall comparison between these two models is provided in order to determine which one is the most accurate.

3. Numerical models

3.1. The Partial Bounce Back model (PBB) [8]

The PBB model is introduced to solve problems with thermal contact resistance between two bodies. It assumes that only a proportion of the thermal energy of the first body can be transmitted to the second, when the remaining energy rebounds towards the first body itself in the opposite direction as shown in Fig. 2. The rebounded proportion is represented by the parameter δ (partial bounce back parameter) which is included between 0 and 1.

In this model, the Thermal Contact Resistance is given by:

$$Rc = \frac{3\delta}{1-\delta} \quad (7)$$

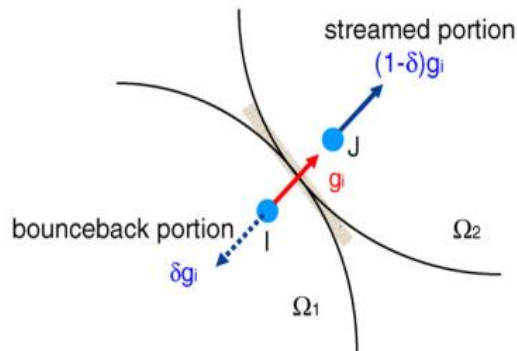


Figure 2. Partial bounce back scheme: [8]

In fact, for a given density function g_i , the proportion $(1-\delta)g_i$ is transmitted from the node I, which belongs to the body 1, to the adjacent node J which belongs to the body 2. The remaining proportion δg_i rebounds to the node I itself.

3.2. The Particle Image model (PI) [10]

This model assumes that both borders in contact are juxtaposed and their distribution functions during the propagation are proportional. For the distribution functions represented in Fig. 3, and in the isotropic case, the proportionality is expressed by two matrix relationships:

$$\begin{pmatrix} f_3 \\ f_6 \\ f_7 \end{pmatrix} = \alpha I_d \begin{pmatrix} g_3 \\ g_6 \\ g_7 \end{pmatrix} \quad \text{and} \quad \begin{pmatrix} g_1 \\ g_5 \\ g_8 \end{pmatrix} = \beta I_d \begin{pmatrix} f_1 \\ f_5 \\ f_8 \end{pmatrix} \quad (8)$$

With :

I_d is the 3×3 identity matrix

f_i : density functions related to the medium 1 for $0 \leq i \leq 8$

g_i : density functions related to the medium 2 for $0 \leq i \leq 8$

In order to evaluate the parameters α and β , we use the following equations:

$$Q_{12} = Q_{21} \quad (9)$$

$$Q_{12} = \frac{\Delta T}{R_c} \quad (10)$$

q_{12} : heat flux transmitted from medium 1 to medium 2, q_{21} : heat flux transmitted from medium 2 to medium 1, ΔT : temperature jump at the contact interface

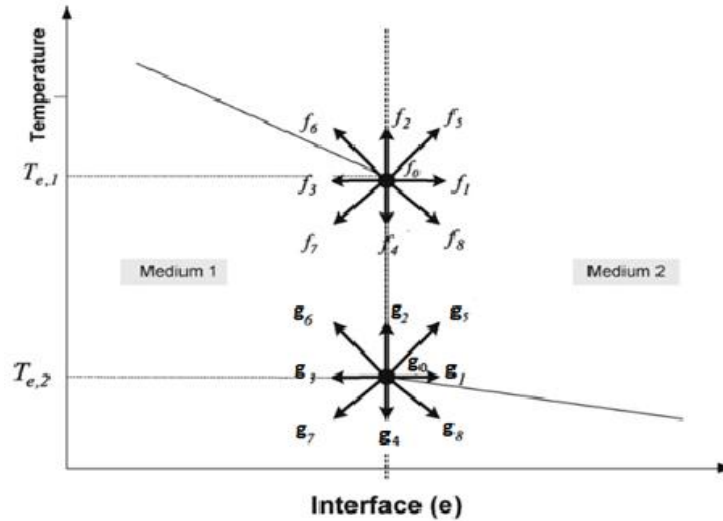


Figure 3. Configuration diagram for the Particle Image model LBM [10]

3.3. Comparisons

The comparisons cover both transient and steady regimes and concern the case represented in Fig. 3, where the contacting media are equally sized rectangular bars with thermal contact resistance at the interface. The bars have the same initial temperature $T_i=0$. During the simulation, the left and

right walls are maintained at different constant temperatures with $T_{\text{left}} = 0$ and $T_{\text{right}} = 1$, when the top and bottom walls are adiabatic to ensure a one-dimensional heat conduction situation.

3.3.1 Transient regime

M.El Ganaoui et al made a comparative study between the two models while validating the PI model and its accuracy [10]. The comparison covered a large range of relaxation time from 0.55 to 1. For $\tau=1$, the two models exhibit accurate agreement with the analytical solution, as shown in Fig. 4. This value of relaxation time ($\tau=1$) corresponds to the hypothesis of the permanent regime introduced by Han et al [8]:

$$f_2 = f_4 = f_2^{\text{eq}} = \frac{1}{6} T \quad (11)$$

Fig. 5 gives the temperature profile at $t=5000$, for $\tau = 0.8$ and $Rc = 1000$. The PBB model exhibits a difference with the analytical solution. This inaccuracy can be explained by the underestimate of the functions f_2 and f_4 in the steady regime. For weak values of the relaxation time, the PI model reaches the analytical solution, when the PBB model show more deviation as show in Fig. 6 and Fig. 7.

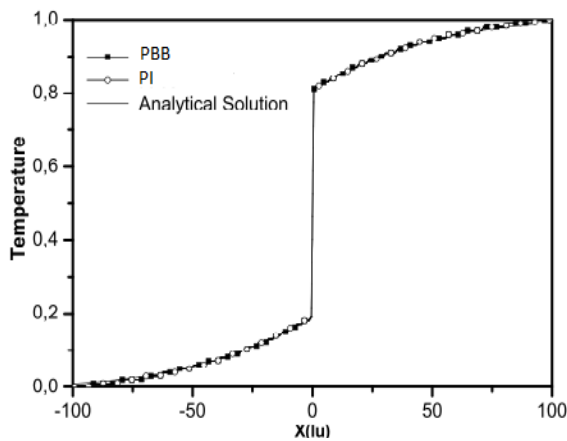


Figure 4. Temperature distribution ($\tau=1, t=10\ 000, Rc=1000$) [10]

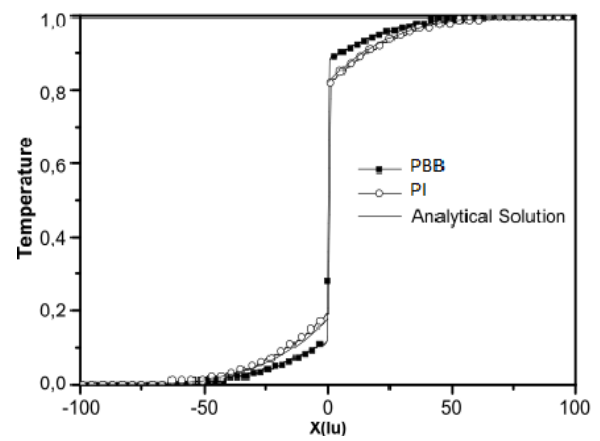


Figure 5. Temperature distribution ($\tau=0.8, t=5\ 000, Rc=1000$) [10]

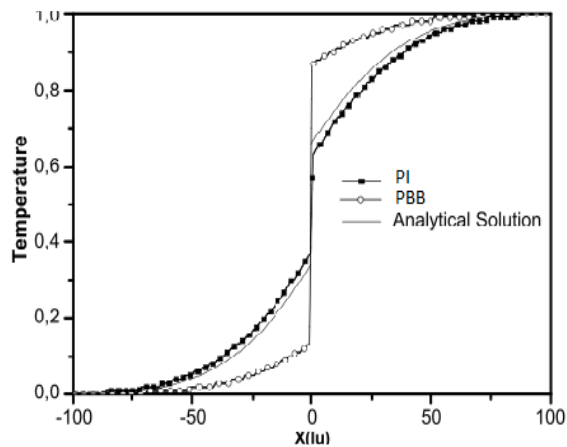


Figure 6. Temperature distribution ($\tau=0.6, t=20\ 000, Rc=1000$) [10]

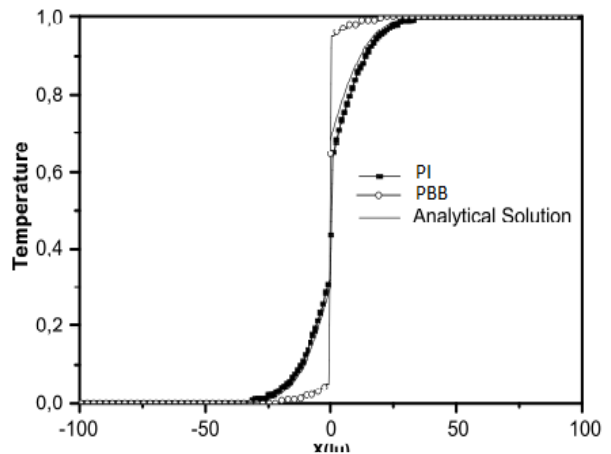


Figure 7. Temperature distribution ($\tau=0.55, t=5\ 000, Rc=1000$) [10]

This study shows that the PBB gives accurate results when $\tau=1$, and exhibits inaccuracy when $0.55 \leq \tau < 1$. In fact, the further the relaxation time is from the value 1, the more inaccurate goes the PBB model, when the PI model still reaches the analytical solution even for low values of relaxation time.

3.3.2 Steady regime

O.El Mhamdi and E.Semma achieved a comparison between the two models in the steady regime. This comparison covered different values of the thermal contact resistance as shown in Fig. 8, Fig. 9, Fig. 10 and Fig.11 [11].

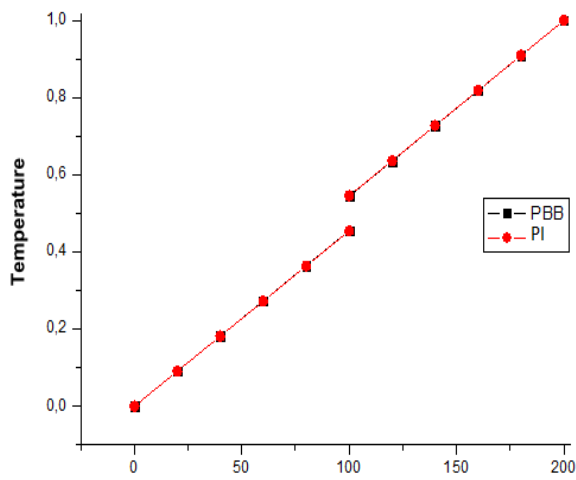


Figure 8. Temperature distribution in space
Rc= 20 [11]

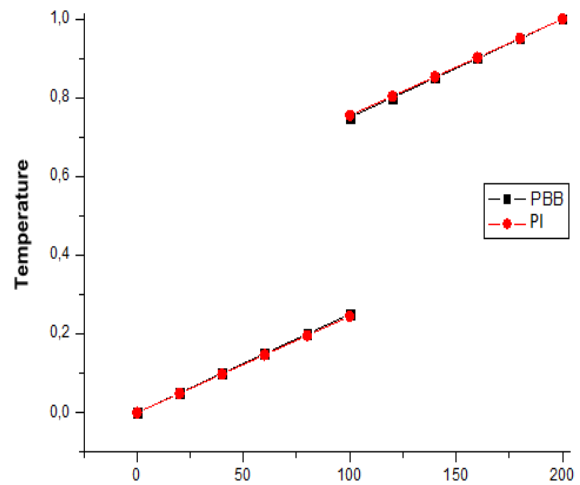


Figure 9. Temperature distribution in space
Rc= 200 [11]

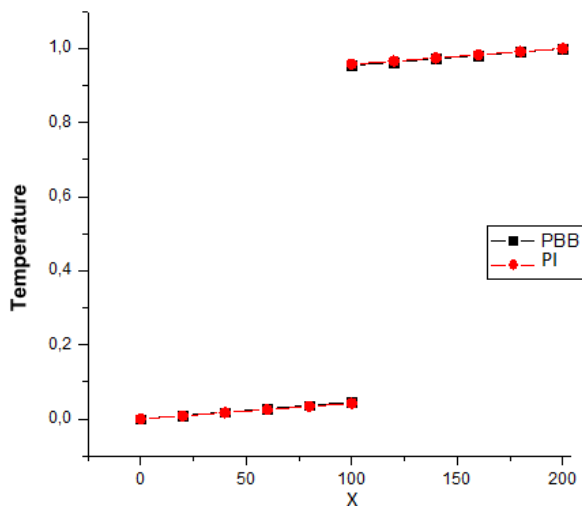


Figure 10. Temperature distribution in space
Rc= 2000 [11]

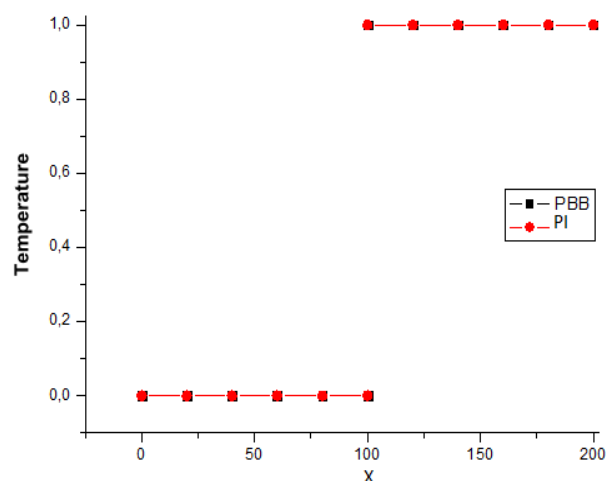


Figure 11. Temperature distribution in space
Rc= ∞ [11]

To sum up this overall comparison, the cases of study discussed have shown that the two models exhibit accurate agreement with the theoretical solution in the steady regime, when the PI model exhibit more accuracy in the transient regime. It can be deduced that the PI model is the most accurate model for solving heat transfer problems with Thermal Contact Resistance. This is why we will be using the PI model in the study of the inclined contact interface.

4. Study of inclined contact interface

4.1. Initial state and boundary conditions

The study area is rectangular 80×40 representing two contacting media following a slope $s=2$ as shown in Fig. 12. Initially ($t=0$), the temperature of the medium 1 equals 0 and the temperature of the medium 2 equals 1. During the simulation, the left side of the medium 1 is maintained at $T_1=0$, while the right side of the medium 2 is maintained at $T_2=1$. With $\Delta x = \Delta y = \Delta t = 1$.

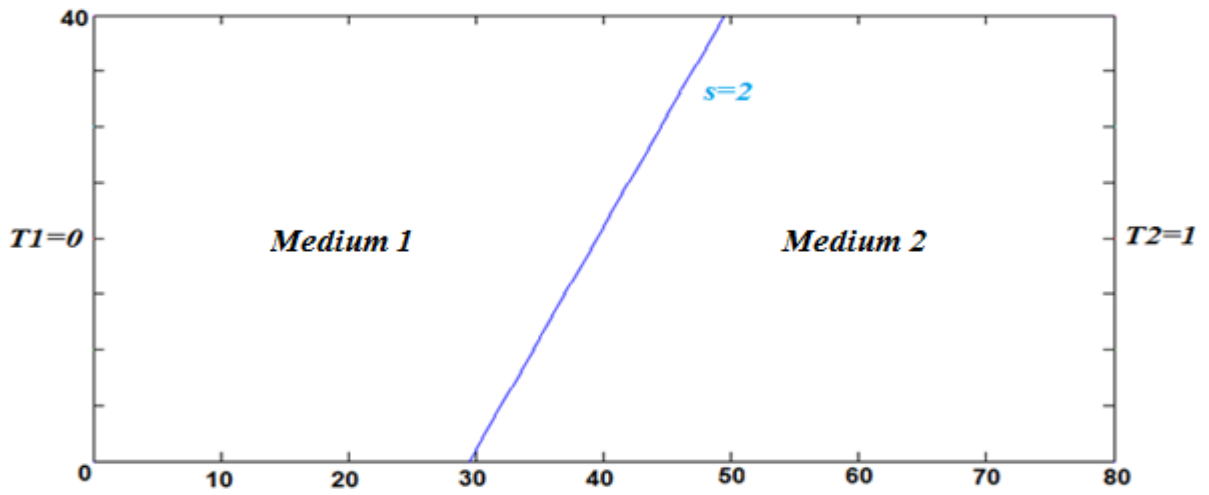


Figure 12. Configuration of inclined contact interface

4.2. Methodology of resolution

The main idea of solving this kind of problems consists in two steps: approaching the points on the contact interface with nodes on the lattice, and calculating the parameters of proportionality α and β at the interface of contact.

4.2.1 Lattice approach

The first step is approaching the points on the contact interface with nodes on the lattice so we can use the LBM method. In fact, each point A with coordinates x_A and y_A belonging to the interface of contact can be approached by a node A' belonging to the lattice as shown in Fig.13. In order to achieve this approach, we can use the following mathematical algorithm:

$$x_A = \begin{cases} i & \text{if } x_A < i+0.5 \\ i+1 & \text{if } x_A \geq i+0.5 \end{cases} \quad y_A = \begin{cases} j & \text{if } y_A < j+0.5 \\ j+1 & \text{if } y_A \geq j+0.5 \end{cases}$$

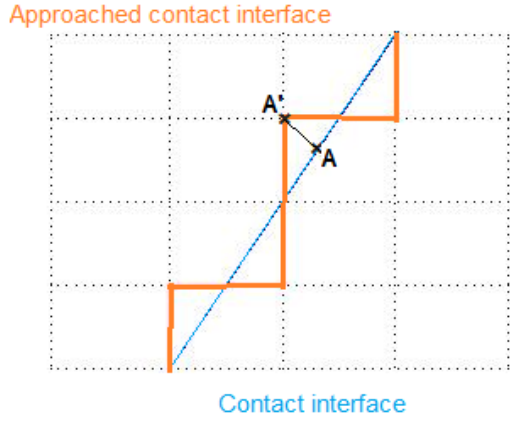


Figure 13. Lattice approach of the contact interface

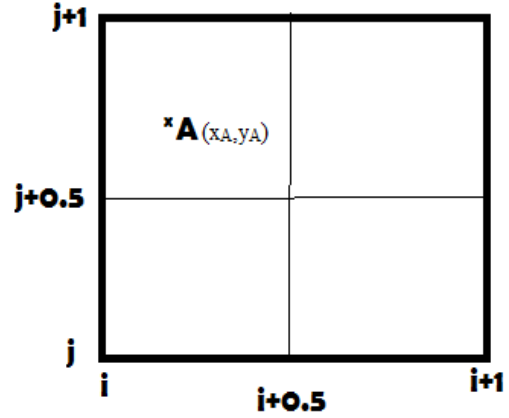


Figure 14. Node approach configuration

4.2.2 Study of nodes

After applying the algorithm all along the contact interface, we find an approached interface as shown in Fig.15. Then, we have to calculate the parameters of proportionality α and β for each node.

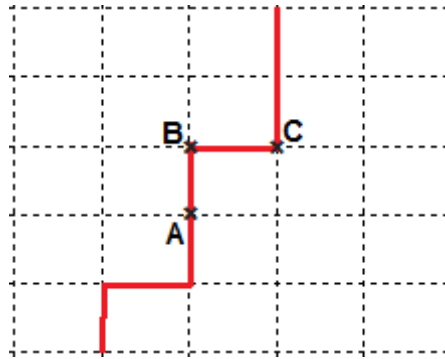


Fig.15. Approached contact interface

There are three cases, and to each case corresponds different parameters α and β as detailed hereafter.

For the node A and similar nodes on the approached contact interface, we have the same case as the configuration represented in Fig.3, where the unknown distribution functions are f_3, f_6, f_7, g_1, g_5 and g_8 . The proportionality between the distribution functions is expressed in eq.(8).

For the node B and similar node, the unknown distribution functions are f_6, g_1, g_4, g_5, g_7 and g_8 . The assumption of proportionality is expressed by the followings relationships:

$$f_6 = \alpha_1 g_6 \quad \text{and} \quad \begin{pmatrix} g_1 \\ g_4 \\ g_5 \\ g_7 \\ g_8 \end{pmatrix} = \beta_1 I_d \begin{pmatrix} f_1 \\ f_4 \\ f_5 \\ f_7 \\ f_8 \end{pmatrix} \quad (12)$$

Finally, for the node C and similar nodes, the unknown distribution functions are f2, f3, f5, f6, f7 and g8. The assumption of proportionality is expressed by the followings relationships:

$$\begin{pmatrix} f2 \\ f3 \\ f5 \\ f6 \\ f7 \end{pmatrix} = \alpha_2 \mathbf{I}_d \begin{pmatrix} g2 \\ g3 \\ g5 \\ g6 \\ g7 \end{pmatrix} \quad \text{and} \quad g8 = \beta_2 g6 \quad (13)$$

With: \mathbf{I}_d is the 5×5 identity matrix.

In order to evaluate the parameters of proportionality α_1 , β_1 , α_2 and β_2 we can use eq.(9) and eq.(10).

4.3. Results and discussion

4.3.1 X-directon flux

In this part, we will have a view over the flow in the X-direction. Fig.16 and Fig.17 represent respectively the temperature distribution for Rc values of 50 and 200, for different values of y (0, 20 and 40). Fig.15 and Fig.16 show that the temperature gap at the contact interface is stable for different values of y. The length difference is due to the inclined interface between the contacting media.

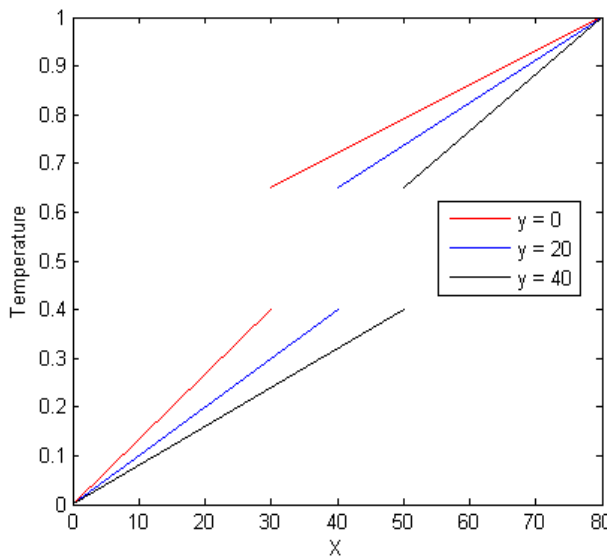


Fig 16. Temperature distribution in X-direction
R=50

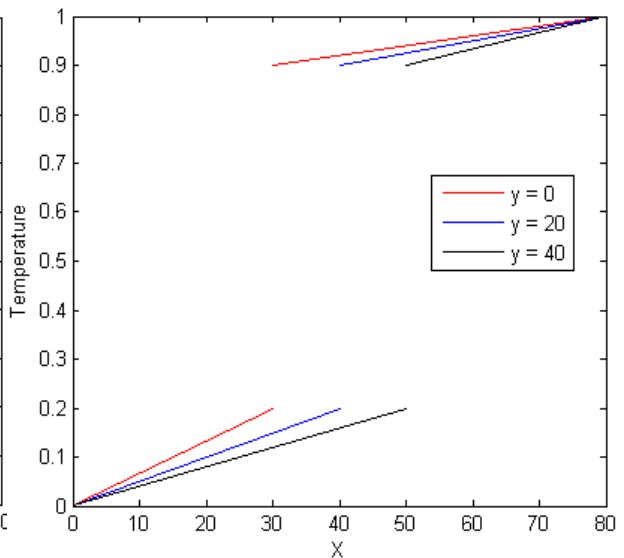


Fig 17. Temperature distribution in X-direction
R=200

4.3.2 Y-directon flux

In this part, we will have a view over the flow in the Y-direction. Fig.18 and Fig.19 represent respectively the temperature distribution for Rc values of 50 and 200, for different values of x (10, 35, 45 and 70).

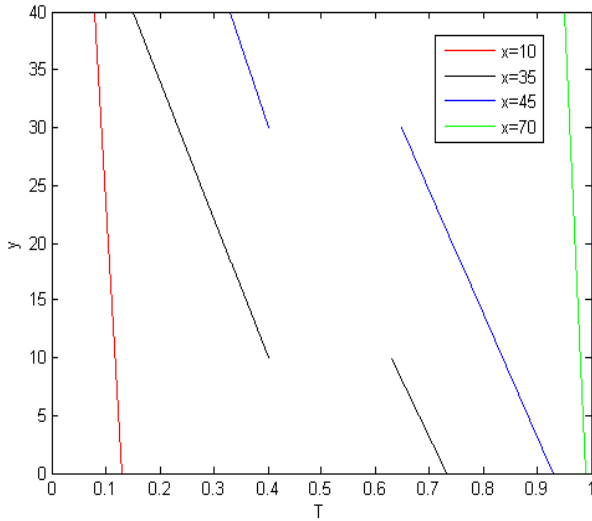


Fig 18. Temperature distribution in Y-direction
R=50

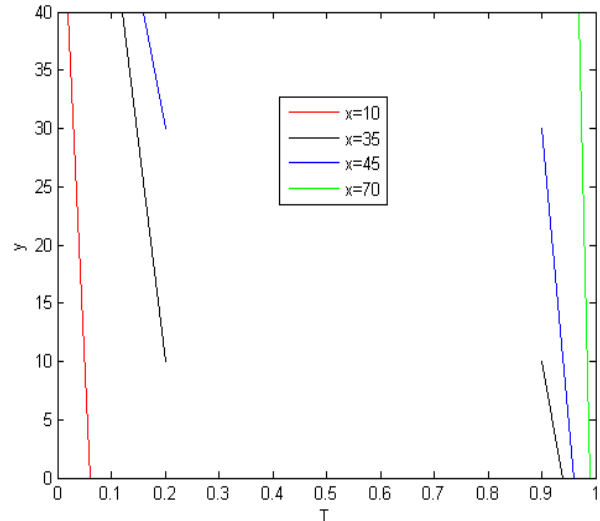


Fig 19. Temperature distribution in Y-direction
R=200

For both R_c values of 50 and 200, the temperature curve is continuous for $x=10$ and $x=70$ because these areas belong to the same medium ($x=10$ belongs to the medium 1 and $x=70$ belongs to the medium 2), while we can notice a discontinuity at $x=35$ and $x=45$ because of the contact interface.

4.3.3 Influence of the thermal contact resistance

In this part, we will evaluate the influence of the thermal contact resistance R_c on heat transfer. Fig.20 represent the temperature distribution in X direction at $y=20$ for different values of R_c (50, 200 and 500) while Fig.21 represent the temperature distribution in Y direction at $x=20$ for the same values of R_c .

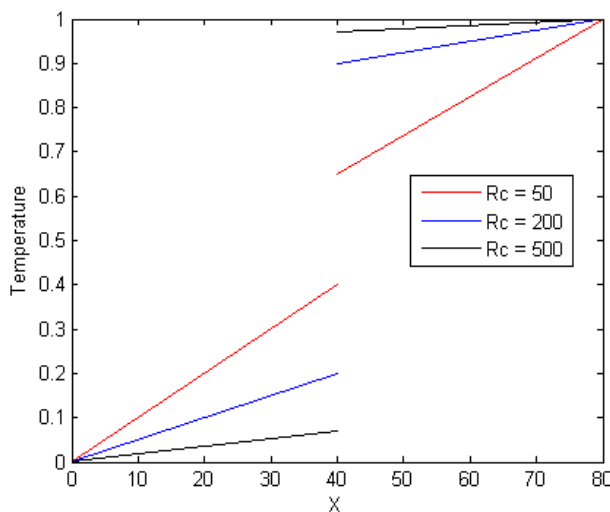


Fig 20. Effect of R_c ($y=20$)

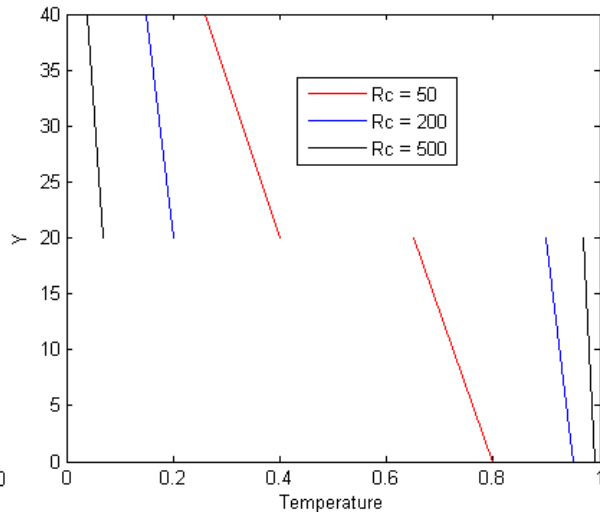


Fig 21. Effect of R_c ($x=20$)

For low values of R_c , the temperature gap is small, and it gets bigger as R_c increases. When R_c equals ∞ , there is no heat flow between the two media. These results can be justified by the effect of TCR, which prevents the perfect heat transfer. The simulated numerical values as well as the theoretical values of the temperature gap at the contact interface are illustrated in Tab. 1, and Fig.22 and Fig.23 represent an overview on the thermal field for $R_c=50$ and $R_c=200$.

Tab.1. Simulated and theoretical temperature gap at the contact interface

R_c	0	50	200	500	2000	∞
Theoretical gap	0	0.26	0.714	0.884	0.962	1
Simulated gap	0	0.253	0.703	0.902	0.978	1

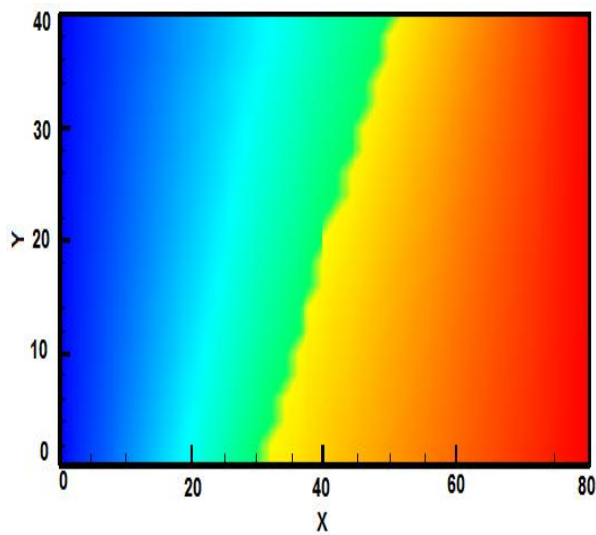
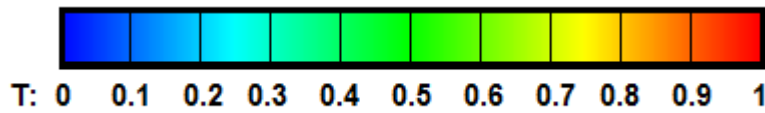


Fig.22. Thermal field, $R_c=50$

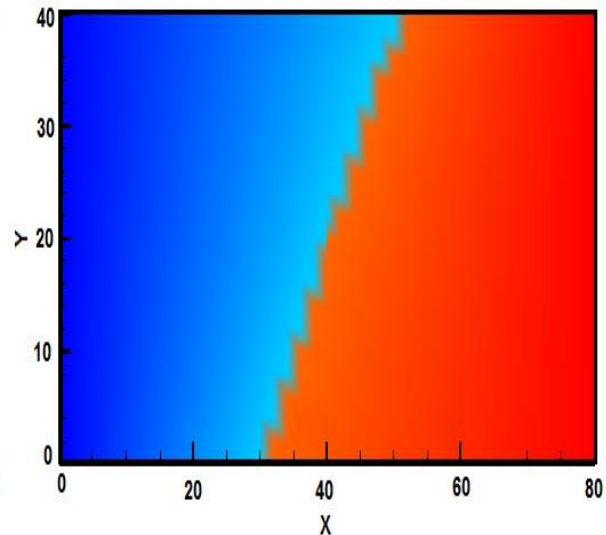


Fig.23. Thermal field, $R_c=200$

5. Conclusion

In this paper, we presented an overall comparison between the PBB model and Pi model and we established a new study of inclined contact interface using Lattice Boltzmann method in order to evaluate a two-dimensional heat transfer. The conclusions are the following:

- 1 – The PI model is accurate for both transient and steady regime, when the PBB model shows inaccuracy in the transient regime. So, the PI model is the most accurate
- 2 – The simulated results show a temperature variation in X and Y directions so the two-dimensional heat transfer is ensured due to the flux at the inclined interface of contact.
- 3 – The simulated results show that the temperature gap at the contact interface is proportional to the thermal contact resistance. (The temperature gap increases when R_c increases and vice versa).

Nomenclature

t	Time	<i>Greek Letters</i>
q	Heat flux	Δx Lattice spacing in x direction
T	Temperature	Δy Lattice spacing in y direction.
R_c	Thermal contact resistance	Δt Time step
		δ Partial bounce back parameter

References

- [1] Guo, Z.L., *et al.*, A lattice BGK model for the Bouessinesq equation, *Internat. J. Numer. Methods Fluids* 39 (2002), pp 325–342.
- [2] Wang, J. *et al.*, A lattice Boltzmann algorithm for fluid solid conjugate heat transfer, *Int. J. Thermal Sci.* 46 (2007), pp 228–234.
- [3] He, X., Luo, L.-S., Theory of the lattice Boltzmann method: From the Boltzmann equation to the lattice Boltzmann equation, *Phys. Rev. E* 56 (1997) , pp 6811–6817.
- [4] He, X., *et al.*, A novel thermal model for the lattice Boltzmann method in incompressible limit, *J. Comput. Phys.* 146 (1998) 282–300.
- [5] D’Orazio, A.Z., *et al.*, Application to natural convection enclosed flows of a lattice Boltzmann BGK model coupled with a general purpose thermal boundary condition, *Int. J. Thermal Sci.* 43 (2004) 575–586.
- [6] Tang, G.H., *et al.*, Thermal boundary condition for the thermal lattice Boltzmann equation, *Phys. Rev. E* 72 (2005), pp 016703
- [7] Huang, H., *et al.*, Thermal curved boundary treatment for the thermal lattice Boltzmann equation, *Int. J. Modern Phys. C* 17 (5) (2006), pp 631–643
- [8] Han, K., *et al.*, Modelling of thermal contact resistance within the framework of the thermal lattice Boltzmann method, *Int. J. Thermal Sci.* 47 (2008), pp 1276–1283.
- [9] Xie, C., *et al.*, Lattice Boltzmann Modeling of Thermal Conduction in Composites with Thermal Contact Resistance. *Communications in Computational Physics*, 17 (2015), pp 1037-1055.
- [10] El Ganaoui, M., *et al.*, Analytical and innovative solutions for heat transfer problems involving phase change and interfaces On the aptitude of the lattice Boltzmann approach for the treatment of the transient heat transfer with crack resistance, *C. R. Mecanique* 340 (2012), pp 518–525.
- [11] El Mhamdi, O., Semma, E., Solving Heat Transfer Problems With Thermal Contact Resistance Using the Lattice Boltzmann Method, *IEEE 4th International conference on Wireless Technologies, embedded and intelligent systems-WITS-2017*, Fez, Morocco, 2017.